

UC Berkeley
SEMM Reports Series

Title

Accuracy Control of a Direct Spectral Method for Nonlinear Elastic Problems

Permalink

<https://escholarship.org/uc/item/1ww6x5gn>

Authors

Wisniewski, Krzysztof

Taylor, Robert

Publication Date

1989-11-01

REPORT NO.
UCB/SEMM-89/21

**STRUCTURAL ENGINEERING
MECHANICS AND MATERIALS**

**ACCURACY CONTROL
OF A DIRECT SPECTRAL METHOD
FOR NONLINEAR ELASTIC PROBLEMS**

BY

K. WIŚNIEWSKI and R. L. TAYLOR

NOVEMBER 1989

**DEPARTMENT OF CIVIL ENGINEERING
UNIVERSITY OF CALIFORNIA
BERKELEY, CALIFORNIA**

ACCURACY CONTROL OF A DIRECT SPECTRAL METHOD FOR NONLINEAR ELASTIC PROBLEMS

by

KRZYSZTOF WISNIEWSKI‡ and ROBERT L. TAYLOR†

ABSTRACT

An accuracy control procedure for nonlinear elastic problems discretized by the direct spectral method is presented. Two forms of the Lax-Richtmyer conditions for convergence are discussed and an error estimation formula suitable for numerical applications is given. It is shown that for an incremental formulation an inconsistency in the approximation scheme may be caused only by an under-representation of global displacements. A procedure to control the solution in the transform space for a Newton - Raphson type algorithm is proposed. An active solution space is defined and an adaptive algorithm is formulated to adjust the spectral representation to changes of this space.

Numerical examples illustrate application of the method to some linear and nonlinear problems for circular elastic rings.

CONTENTS

1. Introduction
 2. Direct Spectral Method
 3. Alternative Form of Lax-Richtmyer Condition
 4. Error Estimation
 5. Consistency for the Incremental Formulation
 6. Space Adaptation
 7. Numerical Examples : Elastic Circular Ring
 - 7.A. Linear Problems
 - 7.B. Non-Linear Problems
 8. Final remarks
- References
Appendix

‡ Polish Academy of Sciences, 00-049 Warszawa, ul. Swietokrzyska 21

† Civil Engineering Department, University of California at Berkeley, Berkeley, CA 94720

ACCURACY CONTROL OF A DIRECT SPECTRAL METHOD FOR NONLINEAR ELASTIC PROBLEMS

by

KRZYSZTOF WISNIEWSKI and ROBERT L. TAYLOR

1. INTRODUCTION

Spectral methods may be used to expand the solution of the differential equations in terms of global basis functions. For many applications spectral methods have the potential for rapid convergence. The methods have been extensively tested within the field of fluid mechanics and have provided primary solution techniques in areas such as simulation of turbulent flows and computation of transition to turbulence, as reported in a recent survey by Hussaini, Kopriva, Patera [1989]. Although problem solutions in solid and structural mechanics are dominated by applications of the finite element method spectral methods have been used successfully to solve many problems. Problems of symmetric bodies subjected to unsymmetric loads seem to be especially well suited for these methods, see Wisniewski, Taylor [1989]

The direct spectral method may be classified as a Galerkin method which uses trigonometric identities and exact integration. Integrals are calculated by reduction of trigonometric polynomials to polynomials of second order for which integrals are exact. Details for this step are included in Section 2.

Several aspects of the method related to convergence, error control and space adaptation are studied in the present paper. The problem of convergence may be treated via the Lax - Richtmyer conditions which impose certain restrictions on the approximation scheme. However, a classical form of these conditions checks the consistency on an exact solution which is unknown for complicated boundary value problems. To alleviate this problem an alternative form of the Lax - Richtmyer conditions is formulated (Section 3) and a simpler form is given later in Section 4. This form provides a measure of error based on an estimation of the residual of the exact equation. In Section 5 an inconsistency of the tangent operator for a direct spectral method is discussed. It is pointed out that the inconsistency is caused only by an incompleteness of the representation for the global displacements. Consequently, the problem of consistency is replaced by the problem of controlling and adjusting the solution space. For cases where loads are represented exactly, the residual of the approximate equilibrium equation is identical to the residual of the exact equation. Hence, convergence to the exact solution is automatically coerced by the Newton - Raphson method. Finally, in Section 6 a space adaptation strategy is described. This strategy determines an active part of the solution space after each step of the Newton - Raphson method and resizes the approximation space as the active space enlarges. Section 7 describes results of numerical calculations on some linear and non-linear test problems..

2. DIRECT SPECTRAL METHOD

The purpose of this chapter is to characterize the direct spectral method as an approximation scheme for partial differential equations. Partially we follow here a description given by Gottlieb and Orszag [1977] and Wisniewski and Taylor [1989].

Let us assume that u is an element of a space \mathbf{K} . The solution of the equation $L u = f$ in domain D belongs to the subspace \mathbf{B} of \mathbf{K} satisfying boundary conditions $B u = 0$ on ∂D . When a boundary value problem is well posed L is a bounded operator from \mathbf{K} to \mathbf{B} .

The formulation of a spectral method involves two steps :

- (i) the choice of an approximation space B_N which is an N-dimensional subspace of B ,
- (ii) the choice of the projection operator P_N of B onto B_N

The operator P_N is used to obtain finite dimensional projections $u_N = P_N u$ and $f_N = P_N f$. An approximation to the governing equation is in the form

$$L_N u_N = f_N \quad (2.1)$$

where an operator L_N from K to B_N is expressed as $L_N = P_N L P_N^{-1}$.

Two types of approximations are used: Galerkin and collocation and each is based on a truncated series representation:

$$u_N(x) = \sum_{n=1}^N a_n t_n(x) \quad (2.2)$$

where $t_n(x)$ are specified linearly independent functions. Usually, Fourier or Chebyshev series are used as a basis of the approximation space.

In a classical Galerkin approximation, the functions $t_n(x)$ must individually satisfy the boundary conditions and the coefficients a_n are determined from the equation :

$$(t_n, L u_N) = (t_n, f), \quad n=1, \dots, N \quad (2.3)$$

with the inner product defined as $(a, b) = \int_D a b dD$.

If $t_n(x)$ do not individually satisfy the boundary conditions then an additional k boundary constraints are imposed as

$$\sum_{n=0}^{N+k} a_n B t_n = 0 \quad (2.4)$$

where $N + k$ is the number of terms in the representation (2.2). The coefficients a_n are determined from the N equations of (2.3) and k equations of (2.4). This method is sometimes also called the tau or Lanczos approximation.

A classical collocation approximation requires the equilibrium equation to be satisfied at $N+1$ collocation points x_i

$$\sum_{n=0}^N a_n t_n(x_i) = u(x_i), \quad i=0, \dots, N \quad (2.5)$$

The direct spectral method is characterized in our work as a Galerkin approximation which is based on Fourier series and an exact integration procedure. It may be used for both linear and non-linear equations.

For linear problems the term $(t_n, L u_N)$ in equation (2.3) is a second order trigonometric polynomial for which exact integrals are known. For incremental nonlinear problems L is a tangent operator and an integration scheme must be specified to deal with trigonometric polynomials of 3rd and higher order in $(t_n, L u_N)$. In the direct method trigonometric identities of the type:

$$\sin \phi_1 \sin \phi_2 = \frac{1}{2} [-\cos (\phi_1 + \phi_2) + \cos (\phi_1 - \phi_2)] \quad (2.6)$$

are used to reduce the order of products in the trigonometric series to polynomials of the second order for which integrals are known.

3. ALTERNATIVE FORM OF LAX - RICHTMYER CONDITION

The Lax - Richtmyer condition introduces notions of consistency and stability which separate factors necessary for the convergence of a solution. A classical form of this condition results from

the following identities:

$$u_N = L_N^{-1} f_N \quad (3.1.a)$$

$$u = (L_N^{-1} L_N) u \quad (3.1.b)$$

$$L_N^{-1} (L u - f) = 0 \quad (3.1.c)$$

If we subtract equation (3.1.b) from equation (3.1.a) and add equation (3.1.c) then after reordering terms we get:

$$u - u_N = L_N^{-1} (L_N - L) u + L_N^{-1} (f - f_N) \quad (3.2)$$

and the following estimation holds:

$$|| u - u_N || \leq || L_N^{-1} || || (L_N - L) u || + || L_N^{-1} || || (f - f_N) || \quad (3.3)$$

with $|| \cdot ||$ denoting a proper norm. Necessary and sufficient conditions for the convergence of u_N to u are formulated as:
the stability condition

$$|| L_N^{-1} || < k \quad , \quad k - \text{constant} \quad (3.4.a)$$

and the consistency conditions

$$\lim_{N \rightarrow \infty} || (L_N - L) u || = 0 \quad (3.4.b)$$

$$\lim_{N \rightarrow \infty} || (f - f_N) || = 0 \quad (3.4.c)$$

The Lax - Richtmyer condition given in Eq. (3.3) has a substantial disadvantage when applied to complicated boundary value problems: an exact form of the solution u is not known and the related term cannot be estimated. Similarly, the consistency condition (3.4.b) also cannot be estimated and the usefulness of this form of the condition is very limited.

An alternative formulation can be obtained when the identities given below are used instead of equations (3.1).

$$u = L^{-1} f \quad (3.5.a)$$

$$u_N = (L^{-1} L_N) u_N \quad (3.5.b)$$

$$L^{-1} (L_N u_N - f_N) = 0 \quad (3.5.c)$$

These identities lead to

$$u - u_N = L^{-1} (L - L_N) u_N + L^{-1} (f - f_N) \quad (3.6)$$

and the subsequent estimation holds:

$$|| u - u_N || \leq || L^{-1} || || (L - L_N) u_N || + || L^{-1} || || (f - f_N) || \quad (3.7)$$

For this formulation the estimation of $|| u - u_N ||$ does not depend on the unknown exact solution u . The alternative consistency condition, to replace equation (3.4.b), may be defined as:

$$\lim_{N \rightarrow \infty} || (L - L_N) u_N || = 0 \quad (3.8)$$

which states that closeness of operators L and L_N should also hold on the approximate solution u_N .

The stability condition, which in the classical formulation was expressed in terms of L_N^{-1} , Eq. (3.4.a), now refers to the operator L^{-1} , which, analogically, must be bounded from above.

4. ERROR ESTIMATION

Consistency and stability of an approximation scheme guarantee convergence as the size of the approximation space goes to infinity. For finite dimensional spaces a distance between the approximate solution and the exact one need to be estimated.

The error defined as $\epsilon_N = u - u_N$ can be expressed as:

$$u - u_N = L^{-1} (f - L u_N) \quad (4.1)$$

obtained by subtraction of equation (3.5.b) from equation (3.5.a). The following estimation holds:

$$\| u - u_N \| \leq \| L^{-1} \| \| (f - L u_N) \| \quad (4.2)$$

These equations are equivalent to the conditions given by equations (3.6) and (3.7) but are more useful in numerical applications.

To estimate $\| L^{-1} \|$ we notice that if the strain energy is positive definite the operator L is bijective and bounded below. Then the inverse operator L^{-1} is bounded from above

$$\| L^{-1} \| < k \quad , \quad k - \text{constant} \quad (4.3)$$

and equation (4.2) may be rewritten as:

$$\| u - u_N \| < k \| (f - L u_N) \| \quad (4.4)$$

The term $(f - L u_N)$ is a residual of the exact differential equations of the problem for the approximate solution u_N .

For many methods of discretization it is not easy to estimate the residual as the derivatives in L are of higher order than derivatives in L_N . For example the finite element approximations are very often based on polynomials of the lowest admissible order and higher order derivatives (than those in the functional) are not immediately accessible. Additional post - processing techniques are necessary (e.g., see Babuska, Miller [1984]). For spectral approximations based on Fourier series which are functions of class C^∞ this problem does not exist.

We conclude this part with some remarks related to evaluation of the solution for space B_N in comparison with the solution for space B_{N+M} , which very often is done when an exact solution is not known. We assume that the same discretization procedure is used to generate equations for two approximation spaces of size N and $N+M$. For the h - version of the finite element method the bigger space may be generated by a uniform subdivision of the original N elements into $N+M$ elements of the same type. For the spectral method (or p - version of FEM) we use approximation functions (polynomials) of order N and $N+M$. The load vectors and the stiffness operators for these spaces are denoted as follows :

$$[f_N, L_N] \text{ for } B_N \quad , \quad [f_{N+M}, L_{N+M}] \text{ for } B_{N+M} \quad (4.5)$$

When a solution for the space B_N is evaluated in space B_{N+M} then the measure of error is defined as:

$$\epsilon_N = u_{N+M} - u_N \quad (4.6)$$

and may be estimated as

$$\epsilon_N \leq \| (f_{N+M} - L_{N+M} u_N) \| \quad (4.7)$$

Decay in this error only shows that both solutions are close to each other but does not guarantee that the solution converges to the exact one. A divergence is caused by the approximation scheme used to generate finite dimensional equations. Low order (for h - version of the FEM only), incomplete approximation functions or numerical integration may render that the consistency condition (3.4.b) or (3.8) fails. It is difficult to check the consistency and therefore different conditions are formulated to assure the convergence. For example, within the finite element method, the usefulness of the so called "patch test" has been acknowledged, see Taylor et al. [1986].

The consistency problem for the direct spectral method will be discussed in the next section.

5. CONSISTENCY FOR THE INCREMENTAL FORMULATION

A question of consistency of the tangent operator for an incremental formulation of nonlinear problems is addressed and a procedure eliminating factors which may cause an inconsistency for the direct spectral method is formulated.

Let us consider an incremental formulation of the nonlinear problem (formulas derived for a circular ring are given in the Appendix). We denote a tangent operator by L_N^i . This operator depends on a known solution $\bar{u} = u_N^i$ where i is an index for the previous iteration. The standard Newton - Raphson procedure is defined by:

$$L_N^i \Delta u_N^{i+1} = R^i \quad (5.1)$$

$$u_N^{i+1} = u_N^i + \Delta u_N^{i+1} \quad (5.2)$$

The residual (unbalanced) forces are given as follows

$$R^i = f_N - L u_N^i \quad (5.3)$$

where L is a nonlinear equilibrium operator in a weak form. For cases with loads exactly represented by a series of size N , i.e. when $f = f_N$, the residual of the approximate equilibrium equation is identical to the residual of the exact equation.

If the method is convergent the residual forces R^i and the error of approximation (the norm of Eq.(5.3) is used in Eq.(4.4)) are minimized. Hence, the convergence to the exact solution is automatically coerced by the Newton - Raphson method.

If the method defined by (5.1) to (5.3) is divergent then an inconsistency in the tangent operator L_N^i must be suspected. This operator depends on the global displacements \bar{u} and, as no numerical integration is used to generate it, the low order or incompleteness of the approximation series for \bar{u} are the only possible source of an inconsistency.

Because the consistency of the tangent operator is difficult to prove a procedure intended to eliminate the underrepresentation factor, which may cause the inconsistency, is proposed.

Firstly, it is assumed that all terms of Δu_N are used to calculate the global displacements \bar{u} . The maximum size of the space for \bar{u} is limited to the size of the space for Δu_N , see (5.2).

Secondly, the representation of the incremental displacements Δu_N is controlled to determine the number of distinct (active) terms of Δu_N .

Thirdly, the size of the active and the approximation space for Δu_N are compared and, if necessary, the approximation space is resized.

In this way the problem of consistency of L_N^i , is reduced to the problem of controlling and adjusting the representation of incremental displacements. Details of the adaptation procedure are given in Section 6.

6. SPACE ADAPTATION

All the space adaptation methods are based on *a posteriori* error estimates. Two basic techniques for such estimates are used in the finite element method: one based on estimates of residuals and another based on interpolation error estimates, Oden et al.[1986], Zienkiewicz et al. [1986].

The proposed space control and adaptation procedure is applied after each load increment. A part of the spectrum which significantly contributes to the solution (active part) is determined and, as necessary, the approximation space is resized.

Let u_N be a solution obtained by means of Eq.(5.1) to (5.3) for a given load f . An active part of this solution is defined as a series for $n = 0, \dots, M$ which guarantees a required accuracy τ . Several measures are used to determine the active part of the solution:

– for residual forces:

$$|| (f - L u_M) || \leq \tau || f || \quad (6.1)$$

$$(u_N, (f - L u_M)) \leq \tau (u_N, f) \quad (6.2)$$

– for displacements:

$$|| u_N - u_M || \leq \tau || u_N || \quad (6.3)$$

– for strain energy:

$$(u_N, f_M) \leq \tau (u_N, f) \quad (6.4)$$

A largest value of M calculated from equations (6.1) to (6.4) is an actual size of the active space.

After the above evaluation, the size of the active space and the approximation space are compared.

1. The approximation space is enlarged if $M \geq N - buffer$. A new size is equal $N = M + buffer$ where the *buffer* denotes an additional set of terms, which are used to avoid recalculation at the same load level for cases when $M = N$. If however $M < N$, i.e. when the buffer diminished only, then the space is resized and the next load step is executed.

2. The approximation space is not changed for $M < N - buffer$.

7. NUMERICAL EXAMPLES : ELASTIC, CIRCULAR RING

7.A. LINEAR PROBLEMS

If we use Fourier representations for the displacement vector \mathbf{u} :

$$\mathbf{u} = \sum_{n=0}^N \mathbf{u}_n t_n \quad (7.1)$$

then the linear elastic stiffness operator L splits into parts L_n related to individual harmonics n . In this case the displacements $\mathbf{u}_n = (w_n, v_n)$ depend only on loads $\mathbf{f}_n = (f_{wn}, f_{vn})$.

Example 7.A.1. Spectral flexibility

Let's assume that the load is a one - parameter function, namely the load is given as $\mathbf{f}_n = (f_{wn}, 0)$. We define a spectral flexibility s_{un} as a ratio:

$$s_{un} = \frac{u_n}{f_{wn}} \quad (7.2.a)$$

where u_n is a component of the displacement vector \mathbf{u}_n . If the operator $L_n = L_n^T$ then the spectral decomposition provides $L_n = U \Lambda U^T$, where Λ is a diagonal matrix of eigenvalues and U is an orthonormal matrix of eigenvectors. The parameters s_{un} are entirely expressed by the eigenvalues and eigenvectors of the operator L_n .

$$\begin{bmatrix} s_{wn} \\ s_{vn} \end{bmatrix} = L_n^{-1} \begin{bmatrix} 1 \\ 0 \end{bmatrix} \quad (7.2.b)$$

A circular, elastic ring under transverse spectral loads given as $f_{wn} = 1.0$ for $n=0, \dots, 100$ is analyzed. Geometrical parameters of the ring are: radius $a = 100.0$, thickness $h = 1.0$, Young's modulus $E = 0.3 \cdot 10^8$. The equations used for the analysis are described in the Appendix.

Results of this analysis (s_{wn} and s_{vn} in Fig. 7.1) indicate a considerable decrease of the amplitudes of each harmonic as n increases. The same property is exhibited by the membrane

forces N_n and the internal moments M_n (Fig. 7.2).

The decreasing spectral flexibility is a quite promising property when loads are represented as infinite series and permits neglecting harmonics with higher numbers.

Example 7.A.2. Pinched ring

This example is to compare the decay of errors of loads and displacements as functions of the number of terms in their spectral representations.

The same ring as in Example 7.A.1 is analyzed. Loads consist of two concentrated forces $P = 1.0$ applied at $\phi = 0^\circ$ and $\phi = 180^\circ$. The exact representation of these loads is an infinite series, obtained from this for the Dirac delta function and additionally rescaled. The following finite series is used in calculations:

$$p_w = q \frac{1}{N+1} \left(1 + \sum_n 2 \cos n\phi \right) , \quad n = 2,4,\dots,N \quad (7.3)$$

Loads calculated from this formula for $q = 1.0$ and $N = 100$ are shown in Fig. 7.3. Results of the analysis obtained for $N = 100$ are shown: displacements w_n, v_n in Fig. 7.4, normalized internal forces and moments N_n, M_n in Fig. 7.5.

The approximation error of the function g by a spectrum consisting of N harmonics is defined as:

$$e = \frac{|| g - g_N ||}{|| g ||} \quad (7.4.a)$$

The mean - square norm based on Fourier coefficients a_n of the function g is defined as:

$$|| g ||^2 = 2 \pi a_0^2 + \pi \sum_{n=1}^N a_n^2 \quad (7.4.b)$$

The norms based on values of g at control points j are defined as:

$$|| g ||_1 = \max | g_j | , \quad || g ||_2^2 = \sum_{j=1}^J g_j^2 \quad (7.4.c)$$

The mean - square errors of p_{wN} related to loads for $N = 1000$ and the mean - square errors of w_N related to the solution for $N = 1000$ are shown in Fig. 7.6. Fig. 7.7 shows errors of the displacements w calculated by Eq. (7.4.c) at uniformly distributed control points within $\phi = 0, \dots, 180$. The errors of displacements w_n decrease much faster than the errors of loads p_{wn} . For example, for $N = 10$ errors of displacement in the defined norms are equal about 0.00001 % while errors of loads are 67.35 %. This indicates that very exact displacements may be obtained even when loads are given by a short series and seem to be unadequately represented.

7.B. NONLINEAR PROBLEMS

Example 7.B.1. Spectral properties of the product operator

Two problems important for nonlinear operators and spectral representations are illustrated. These are a boundedness of the product series for spectra of different profiles and an expansion of the product for a simple iterative procedure.

Let O and \bar{O} denote nonlinear operators acting on functions and their spectral representations, respectively. We assume that the following relations, between functions a, b, c and their

series representations, hold:

$$\text{functions} : a, b ; c = O(a, b) \quad (7.5)$$

$$\text{series} : a_n, b_n ; c_m = \bar{O}(a_n, b_n) \quad (7.6)$$

for $n=0, \dots, N$ and $m=0, \dots, M$

Profiles of a_n and b_n determine a profile of c_n . Here, we calculate c_n only for a simple nonlinear operator, namely when O is a product operator:

$$O(a, b) = a * b \quad (7.7)$$

For series representations operator O is replaced by \bar{O} which in an additive form is:

$$\bar{O}(a_i, t_i^1, b_j, t_j^2) \equiv a_i b_j \quad 0.5(t_i^3 \pm t_j^4) \quad (7.8)$$

where $l=i+j$ and $k=i-j$. Trigonometric functions t^3, t^4 can be expressed by trigonometric functions t^1, t^2 according to standard trigonometric identities (e.g. (2.6)).

In calculations we assume that $a_n = b_n$, i.e. \bar{O} is a square operator. The spectrum a_n is taken as a constant ($a_n = 1.0$), linear ($a_n = 1.0/n$) and quadratic ($a_n = 1.0/n^2$) function of n . Calculations are performed for $N = 100$ and results are presented in Fig. 7.8. The product consists of harmonics with indices up to $2N$. Results for the constant spectrum bound the results for the linear and quadratic spectra.

If the square operator is used repeatedly, as when solving nonlinear equations, the spectral representation expands. For the iteration procedure defined as:

$$f^i = f^{i-1} * f^{i-1} \quad (7.9)$$

with

$$f^{i-1} = \sum_{n=0}^{N_{i-1}} a_n^{i-1} \cos n \phi \quad (7.10)$$

(i is an index of iteration) the result may be written as:

$$f^i = \sum_{n=0}^{N_i} a_n^i \cos n \phi = \alpha_i \sum_{n=0}^{N_i} b_n^i \cos n \phi \quad (7.11)$$

where $\alpha_i = (\alpha_{i-1})^2 \beta_i$, $\beta_i = \max a_n^i$, $N_i = N_0 i^2$ and b_n^i is the normalized a_n^i .

In our calculations the starting values for the iteration are chosen as:

$$a_n^0 = 1.0, \quad n = 0, \dots, N_0, \quad N_0 = 10, \quad \alpha_0 = 1.0 \quad (7.12)$$

Normalized results for iterations $i = 0, \dots, 4$ are shown in Fig. 7.9, and values of β_i and N_i are placed in Table 7.1. A number of harmonics involved N_i and a value of α_i increases for each iteration and for $i = 4$ we have:

$$N_4 = 160, \quad \alpha_4 = (\alpha_0)^{16} (\beta_1)^8 (\beta_2)^4 (\beta_3)^2 \beta_4 \quad (7.13)$$

Thus, in general use of product operators and iterative solutions leads to rapidly expanding number of terms. In applications to problem solution this is balanced by other considerations as shown next.

Example 7.B.2. Nonlinear analysis for self-equilibrating loads

Application of the product operator presented in Example 7.B.1 using Fourier series to a geometrically nonlinear analysis, does not require an approximation space of excessive size. A reasonable size of the approximation space is preserved because the tendency to expand the representation is moderated by the decreasing spectral flexibility.

A problem similar to the one described here was studied by Seide and Jamjoom [1974]. They analyzed a circular ring subjected to forces:

$$p_w = \alpha (1 + q \cos 2\phi) , \quad q = 1.0, 0.1, 0.01, 0.001 \quad (7.14)$$

In our analysis we assume that p_w does not change direction during the deformation. Seide and Jamjoom considered the following forces and used a completely different method of solution. The analysis is based on the nonlinear equations for moderate rotations of rings summarized in the Appendix. An approximation space of harmonics $n = 0, \dots, 9$ is used.

The data is as follows : radius $a = 100.0$, thickness $h = 1.0$, Young's modulus $E = 0.12 \cdot 10^8$. The dimensionless parameters are: $\frac{a}{h} = 100.0$ and $\frac{E I}{a^3} = 1.0$.

For a uniform axisymmetric load, i.e. when $q = 0.0$ in Eq.(7.14), the critical bifurcation load is

$$\alpha_{cr} = 4 \frac{E I}{a^3} \quad (7.15)$$

For the given data $\alpha_{cr} = 4.0$.

The load - displacement curves for w at point $\phi = 0^\circ$ are presented in Fig. 7.10. It can be observed that solutions approach the asymptotic line $\alpha = 4.0$. as $q \rightarrow 0$. The performance of the direct spectral algorithm was very good, especially in the corner of the curve for $q = 0.001$ where the solution exhibits a strongly nonlinear behavior. Several displacement patterns of the ring for different load levels (for $q = 0.001$) are shown in Fig. 7.11., while their spectral representations are given in Fig. 7.12.

The nonlinearity of the equations results in an increased number of harmonics with non-zero coefficients, as explained in the previous example. However, as is evident from Fig. 7.12, their amplitudes decrease very rapidly and influence of the harmonics higher than 4 is negligible. This results from the fact that the elastic stiffness matrix with decreasing spectral flexibility (shown in Examples 7.A.1 and 7.A.2) compensates for the tendency of the initial stress and initial displacement matrices to expand the number of significant harmonics.

Example 7.B.3. Nonlinear analysis for a sinusoidal load

In this example we consider a circular ring with the same properties as in Example 7.A.1. Loads are given by the series

$$p_w = q \frac{2}{\pi} \left[1 - \sum_{n=2}^N \frac{2}{(n-1)(n+1)} \cos n\phi \right] \quad (7.16)$$

which as N tends to infinity converges to the function $\sin \phi$ and has a period π for even values of n .

The load for series (7.16) and $n = 0, \dots, 50$ is shown in Fig. 7.13. Note that the harmonic $n = 1$ is excluded as would lead to a non self-equilibrated solution. The first 28 harmonics constitute more than 99% of the total value of the load function. Analyzing the displacements obtained from a linear analysis it was found that for the first 6 harmonics the error, relative to the solution for 50 harmonics, is smaller than 0.1% .

The analysis is based on nonlinear equations which include effects for moderate rotations of the ring, see the Appendix. Calculations were continued until points under maximums of the loads ($\phi = 90^\circ$ and $\phi = 270^\circ$) came into contact. The tolerance parameter to control convergence of the Newton - Raphson method was set to 10^{-7} .

In the first step calculations were performed for $N = 50$ to obtain reference values. The load - displacement curve is presented in Fig. 7.14. The w - displacement for different load values is

shown in Fig. 7.15. Spectral representation for the w - displacements are given in Fig. 7.16, Equations (6.1) to (6.4) were used to monitor the active part of the solution. Norms in the equations (6.1) and (6.3) were specified as the mean - square norms defined by Eq. 7.4.b. The tolerance τ was set to 10^{-3} . The active space consisted of 6 harmonics throughout the entire analysis.

Later, the same problem was analyzed using the space adaptation strategy described in Section 6. The initial number of harmonics was $N = 6$ and the buffer was 2 harmonics. The solution space was not resized and the results obtained are identical to those for the 50 harmonic model.

8. FINAL REMARKS

This paper provides some results illustrating convergence, error control and adaptivity properties of the direct spectral method.

Several examples are solved to assess performance of the method in modeling of linear and nonlinear behavior of circular rings subjected to static loads. In all examples a dual representation of the solution (in physical and transform space) are monitored.

It is found that for linear cases the spectral flexibility decreases considerably for harmonics with higher harmonic numbers. This feature is very important in cases where loads are represented as infinite or non-decaying series.

For nonlinear applications with this type of loading the size of the active solution space is much smaller that one would expect from the spectral properties of the product operator. The computed examples show that the solution space does not expand significantly as compared to the space of a corresponding linear problem. This rapid convergence is attributed to the decreasing spectral flexibility.

An adaptive strategy, which controls the resizing of the solution space, is implemented. Comparisons with solutions for a full space indicate that high accuracy is preserved for the given definition of the active space. The adaptive strategy improves the effectiveness of the formulation and is especially important for practical applications of the spectral method.

REFERENCES

- BABUSKA I., MILLER A. : "The post-processing approach in the finite element method"
Int. J. Numer. Meth. Engng, Vol. 20, pp. 1085-1109 and 1111-1129 (1984)
- BRUSH, D.O., ALMROTH, B.O. : "Buckling of bars, plates and shells" ,
McGraw-Hill, Inc. (1975)
- GOTTLIEB, D.O., ORSZAG, S.A. : "Numerical Analysis of Spectral Methods : Theory and Applications"
SIAM, Philadelphia (1977)
- HUSSAINI, M.Y., KOPRIVA D.A., PATERA A.T. : "Spectral collocation methods".
Applied Numerical Mathematics, 5, pp. 177-208 (1989)
- ODEN, J.T., DEMKOWICZ, L., STROUBOULIS, T., DEVLOO, P. : "Adaptive methods for problems in solid and fluid mechanics" ,
in "Accuracy estimates and adaptive refinements in finite element computations" , eds. I. Babuska I., O.C. Zienkiewicz, J. Gago, E.R de A. Oliveira , J. Wiley & Sons Ltd. , pp.

249-279 (1986)

SEIDE, P., JAMJOOM, T.M.M. : "Large deformations of circular ring under nonuniform normal pressure",
ASME, J. Appl. Mech. , Vol. 41, pp. 192-196 (1974)

TAYLOR R.L. , SIMO J.C. , ZIENKIEWICZ O.C. , CHAN A.C.H. : "The patch test - a condition for assessing FEM convergence",
Int. J. Num. Meth. Engng. , Vol. 22 , pp. 39-62 (1986)

WISNIEWSKI, K. , TAYLOR, R.L. : "Direct spectral method for the stability analysis of cylindrical shells",
Report UCB/SEMM-89/3, (January 1989), submitted for publication in International Journal of Numerical Methods in Engineering.

ZIENKIEWICZ, O.C. , CRAIG, A. : "Adaptive refinement, error estimates, multigrid solution, and hierarchic finite element method concepts",
in "Accuracy estimates and adaptive refinements in finite element computations" , eds. I. Babuska I., O.C. Zienkiewicz, J. Gago, E.R de A. Oliveira , J. Wiley & Sons Ltd. , pp. 25-59 (1986)

APPENDIX. RING EQUATIONS AND INCREMENTAL DESCRIPTION OF DEFORMATION

Governing equations for circular rings based on the Kirchhoff type hypothesis and on the assumption about moderate rotations of the ring are presented by Brush, Almroth [1975].

For this theory measures of strain and changes of curvature are obtained from the Green strain tensor and are given by:

$$\gamma = \theta + \frac{1}{2} \beta^2 \quad , \quad \kappa = \frac{\beta'}{a} \quad (\text{A.1})$$

with $\theta = \frac{v' + w}{a}$ and $\beta = \frac{v - w'}{a}$ with transverse displacements w , tangent displacements v and $()' = \frac{d}{d\phi} ()$; where a denotes a radius of the undeformed ring.

For a ring in equilibrium under external dead loads f_w the virtual work principle may be expressed as:

$$\int_0^{2\pi} [N \delta\gamma + M \delta\kappa] d\phi = \int_0^{2\pi} f_w \delta w d\phi \quad (\text{A.2})$$

where N , M are symmetric Lagrangean measures of internal forces and moments related to the second Piola - Kirchhoff stress tensor and $\delta()$ denotes a variation.

Applying Stokes theorem to (A.2) we obtain the equilibrium equation:

$$a N' + M' - a N \beta = 0 \quad (\text{A.3.a})$$

$$M'' - a N - a (N \beta)' = f_w a^2 \quad (\text{A.3.b})$$

The strains are assumed to be small and the 'first' approximation of the strain energy Σ for a ring is defined as:

$$\Sigma = \frac{EA}{2} a \int_0^{2\pi} \gamma^2 d\phi + \frac{EI}{2} a \int_0^{2\pi} \kappa^2 d\phi \quad (\text{A.4})$$

where EA , EI are the flexural and the bending stiffness, respectively.

The constitutive relations obtained from the energy Σ have the uncoupled forms

$$N = EA \gamma \quad , \quad M = EI \kappa \quad (A.5)$$

We next deduce incremental formulas which will be used to generate basic matrices of the problem.

We consider the virtual work principle (A.2) for a ring in equilibrium under external surface loads f_w and internal forces and moments N, M . We introduce incremental relations for the displacement vector \mathbf{u} and the load vector f_w as

$$\mathbf{u} = \bar{\mathbf{u}} + \Delta \mathbf{u} \quad , \quad f_w = \bar{f}_w + \Delta f_w \quad (A.6)$$

where known quantities are marked by a bar. The corresponding increments for measure of strains, change of curvatures, internal forces and moments may be expressed as:

$$\Delta \gamma = \gamma - \bar{\gamma} \quad , \quad \Delta \kappa = \kappa - \bar{\kappa} \quad (A.7.a)$$

$$\Delta N = N - \bar{N} \quad , \quad \Delta M = M - \bar{M} \quad (A.7.b)$$

Since $\bar{\mathbf{u}}$ is known the variation of \mathbf{u} is replaced by a kinematically admissible variation of $\Delta \mathbf{u}$ i.e. $\delta \mathbf{u} = \delta(\Delta \mathbf{u})$. Similar relations hold for measures : $\delta \gamma = \delta(\Delta \gamma)$ and $\delta \kappa = \delta(\Delta \kappa)$.

Let us split $\Delta \gamma$ and ΔN into linear (LN) and nonlinear (NL) parts, with respect to the increments of the displacement vector. Accordingly,

$$\Delta \gamma = \Delta \gamma^{LN} + \Delta \gamma^{NL} \quad (A.8.a)$$

$$\Delta N = \Delta N^{LN} + \Delta N^{NL} \quad (A.8.b)$$

Hence, in view of incremental quantities defined above, the potential energy may be expressed as:

$$\delta P = \delta P_1 + \delta P_2 + \delta P_3 + \delta P_4 = 0 \quad (A.9)$$

and differentials are defined as follows:

$$\delta P_1 = \int_0^{2\pi} \left[\bar{N} \delta(\Delta \gamma^{LN}) + \bar{M} \delta(\Delta \kappa) - \bar{f}_w \delta(\Delta w) - \Delta f_w \delta(\Delta w) \right] d\phi$$

$$\delta P_2 = \int_0^{2\pi} \left[\bar{N} \delta(\Delta \gamma^{NL}) + \Delta N^{LN} \delta(\Delta \gamma^{LN}) + \Delta M \delta(\Delta \kappa) \right] d\phi$$

$$\delta P_3 = \int_0^{2\pi} \left[\Delta N^{LN} \delta(\Delta \gamma^{NL}) + \Delta N^{NL} \delta(\Delta \gamma^{LN}) \right] d\phi$$

$$\delta P_4 = \int_0^{2\pi} \left[\Delta N^{NL} \delta(\Delta \gamma^{NL}) \right] d\phi$$

The virtual work of external and internal forces for a known configuration is expressed as:

$$\delta R = \int_0^{2\pi} \left[\bar{N} \delta(\Delta \gamma^{LN}) + \bar{M} \delta(\Delta \kappa) - \bar{f}_w \delta(\Delta w) \right] d\phi \quad (A.10)$$

If a known configuration is an equilibrium configuration then $\delta R = 0$ and we obtain the virtual work principle. Otherwise (A.10) is treated as a virtual work of unbalanced internal forces and moments.

In the process of linearization δP_3 and δP_4 are omitted. Additionally, δP_2 is split by introducing $\Delta \gamma^{LN} = \Delta \gamma^o + \Delta \gamma^L$ where $\Delta \gamma^o$ depends only on $\Delta \mathbf{u}$ while $\Delta \gamma^L$ depends on $\bar{\mathbf{u}}$ and on $\Delta \mathbf{u}$. In a similar way we treat ΔN^{NL} obtaining the following expressions for the second differential:

$$\delta P_2 = \delta P_2^o + \delta P_2^L + \delta P_2^L + \delta P_2^L + \delta P_2^{NL} \quad (A.11)$$

with

$$\begin{aligned}\delta P_2^{\sigma\sigma} &= \int_0^{2\pi} \left[\Delta N^\sigma \delta(\Delta\gamma^\sigma) + \Delta M \delta(\Delta\kappa) \right] d\phi \\ \delta P_2^{\sigma L} &= \int_0^{2\pi} \left[\Delta N^\sigma \delta(\Delta\gamma^L) \right] d\phi \quad , \quad \delta P_2^{L\sigma} = \int_0^{2\pi} \left[\Delta N^L \delta(\Delta\gamma^\sigma) \right] d\phi \\ \delta P_2^{LL} &= \int_0^{2\pi} \left[\Delta N^L \delta(\Delta\gamma^L) \right] d\phi \quad , \quad \delta P_2^{NL} = \int_0^{2\pi} \left[\Delta \bar{N} \delta(\Delta\gamma^{NL}) \right] d\phi\end{aligned}$$

Standard basic matrices are derived from the following parts of δP_2 :

$$\begin{aligned}\delta P_2^{\sigma\sigma} &\rightarrow [K_\sigma] \Delta q \\ \delta P_2^{\sigma L} + \delta P_2^{LL} + \delta P_2^{L\sigma} &\rightarrow [K_u] \Delta q \\ \delta P_2^{NL} &\rightarrow [K_\sigma] \Delta q\end{aligned}\tag{A.12}$$

where $[K_\sigma]$ is an elastic stiffness matrix, $[K_\sigma]$ is an initial stress matrix, $[K_u]$ is an initial displacement matrix, Δq is an increment of the displacement vector.

Table 7.1. Results of the iteration procedure

i	β_i	N_i
0	1.0	10
1	11.0	20
2	7.8554	40
3	11.0954	80
4	15.2696	160

FIGURES

Example 7.A.1. Unit spectral loads

Fig.7.1. Spectral flexibility s_{wn} and s_{vn} of a circular ring under loads $p_{wn} = 1.0$.

Fig.7.2. Spectra of membrane forces N_n and internal moments M_n of a circular ring under loads $p_{wn} = 1.0$.

Example 7.A.2. Pinched ring

Fig.7.3. Loads $p_w = \frac{1}{101} (1 + \sum_n 2 \cos n\phi)$, $n=2,4,\dots,100$ modeling two concentrated forces.

Fig.7.4. Displacements w_n and v_n of a pinched ring. $N = 100$.

Fig.7.5. Normalized membrane forces N_n and internal moments M_n of a pinched ring. $N = 100$.

Fig.7.6. Spectral errors of loads and displacements w for two concentrated forces related to $N = 1000$.

Fig.7.7. Errors of displacements w for two concentrated forces related to $N = 1000$ computed at control points.

Example 7.B.1. Spectral properties of the product operator

Fig.7.8.a. Spectrum of the product $a_n \sin n\phi * a_m \sin m\phi$ for $n,m = 0,100$ for constant, linear and quadratic a_n .

Fig.7.8.b. Spectrum of the product $a_n \cos n\phi * a_m \cos m\phi$ for $n,m = 0,100$ for constant, linear and quadratic a_n .

Fig.7.8.c. Spectrum of the product $a_n \sin n\phi * a_m \cos m\phi$ for $n,m = 0,100$ for constant, linear and quadratic a_n .

Fig.7.9. Normalized spectra for $f^i = f^{i-1} * f^{i-1}$ with $i = 1,2,3,4$. $f^0 = \sum_{n=0}^{10} 1 \cos n\phi$.

Example 7.B.2. Nonlinear analysis for self-equilibrating loads

Fig.7.10. Load - displacement curves for ring (point $\phi = 0^\circ$) under loads $p_w = \alpha (1 + q \cos 2\phi)$, $q = 1.0, 0.1, 0.01, 0.001$.

Fig.7.11. Displacements w of ring under loads $p_w = \alpha (1 + q \cos 2\phi)$ for $q = 0.001$.

Fig.7.12. Spectral representations of displacements w of ring under loads $p_w = \alpha (1 + q \cos 2\phi)$ for $q = 0.001$.

Example 7.B.3. Nonlinear analysis for a sinusoidal load

Fig.7.13. Loads $p_w \approx \sin\phi$ for $0 \leq \phi \leq \pi$.

Fig.7.14. Load - displacement w curves for ring under loads $p_w \approx \sin\phi$. Points $\phi = 0^\circ$ and $\phi = 90^\circ$.

Fig.7.15. Displacements w of ring under loads $p_w \approx \sin\phi$.

Fig.7.16. Spectral representation of displacements w_n of ring under loads $p_w \approx \sin\phi$.

FIGURES

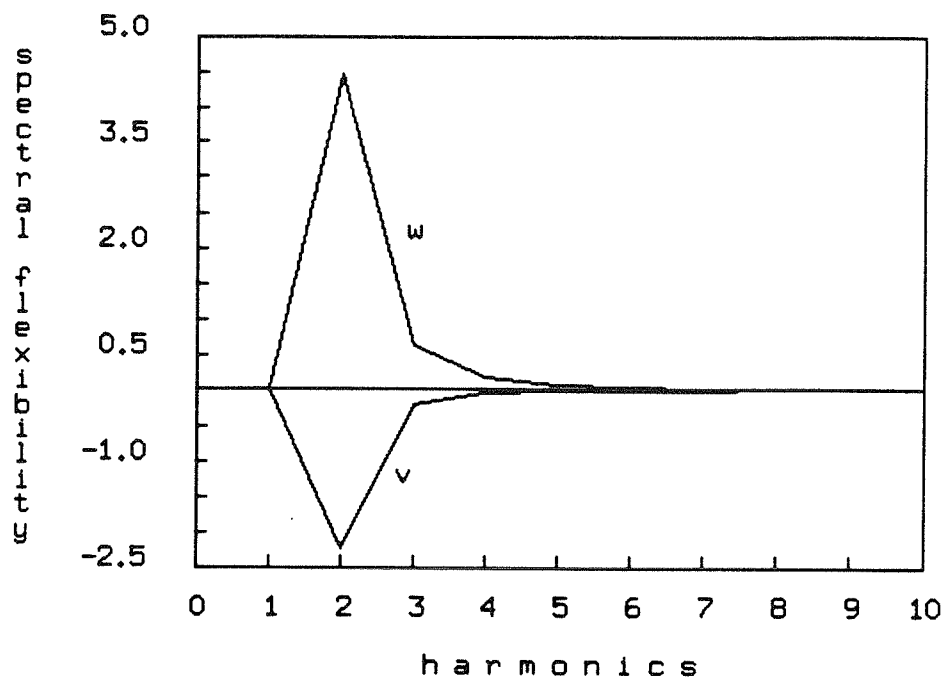


Fig.7.1. Spectral flexibility s_{wn} and s_{vn} of a circular ring under loads $p_{wn} = 1.0$.

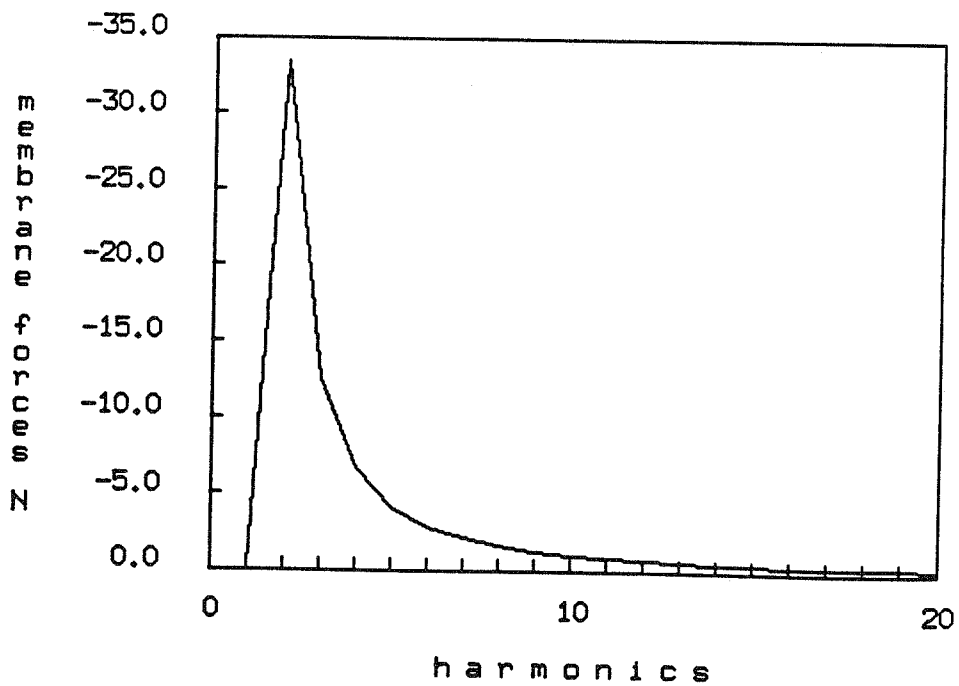


Fig.7.2.a. Spectrum of membrane forces N_n of a circular ring under loads $p_{wn} = 1.0$.

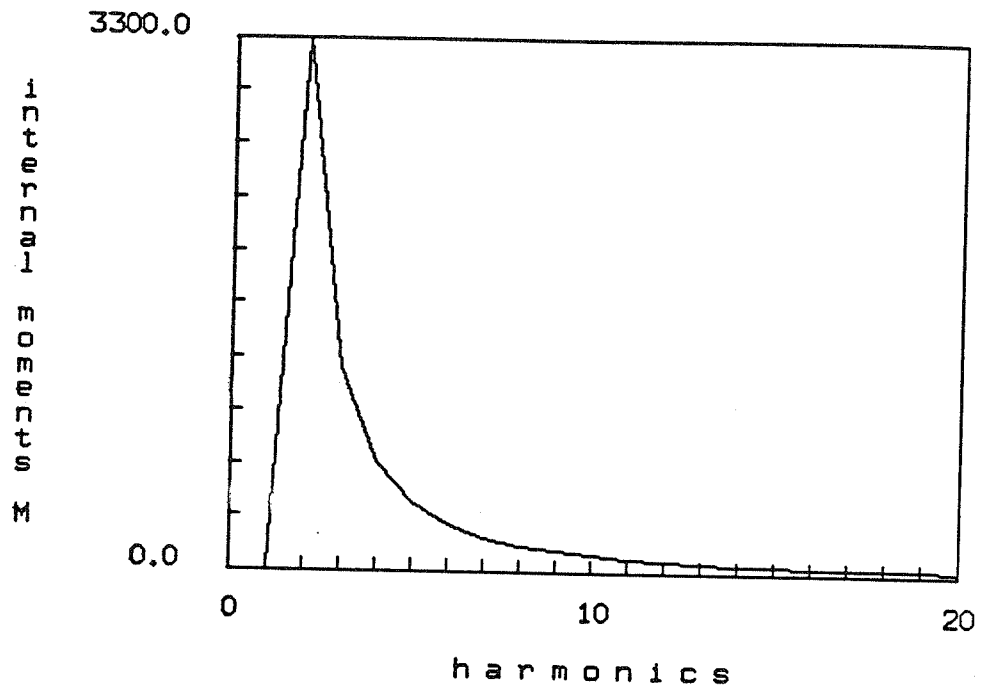


Fig.7.2.b. Spectrum of internal moments M_n of a circular ring under loads $p_{wn} = 1.0$.

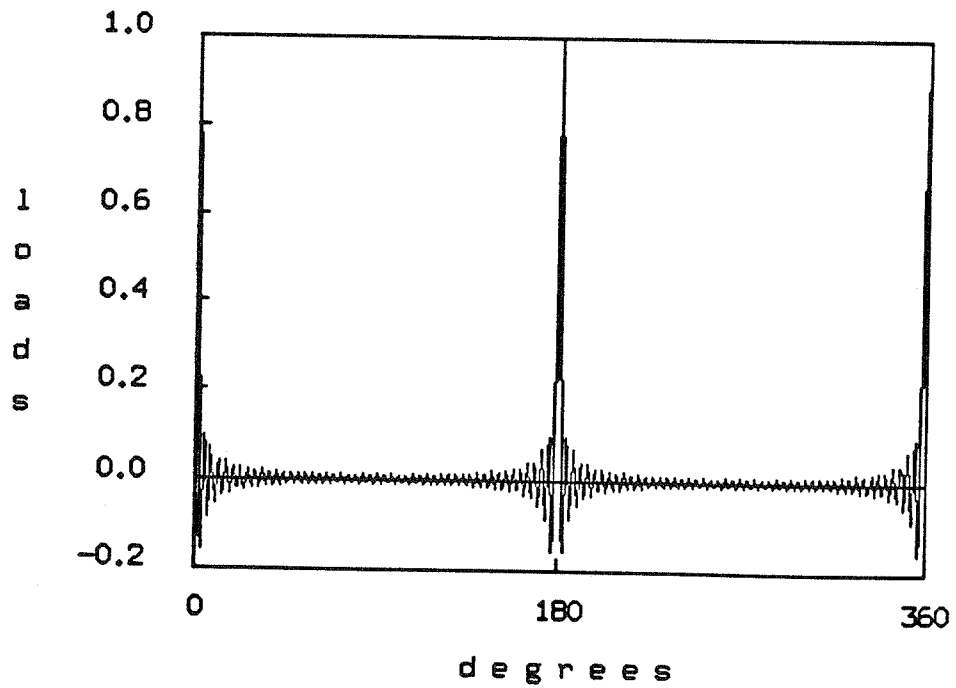


Fig.7.3. Loads $p_w = \frac{1}{101} (1 + \sum_n 2 \cos n\phi)$, $n=2,4,\dots,100$ modeling two concentrated forces.

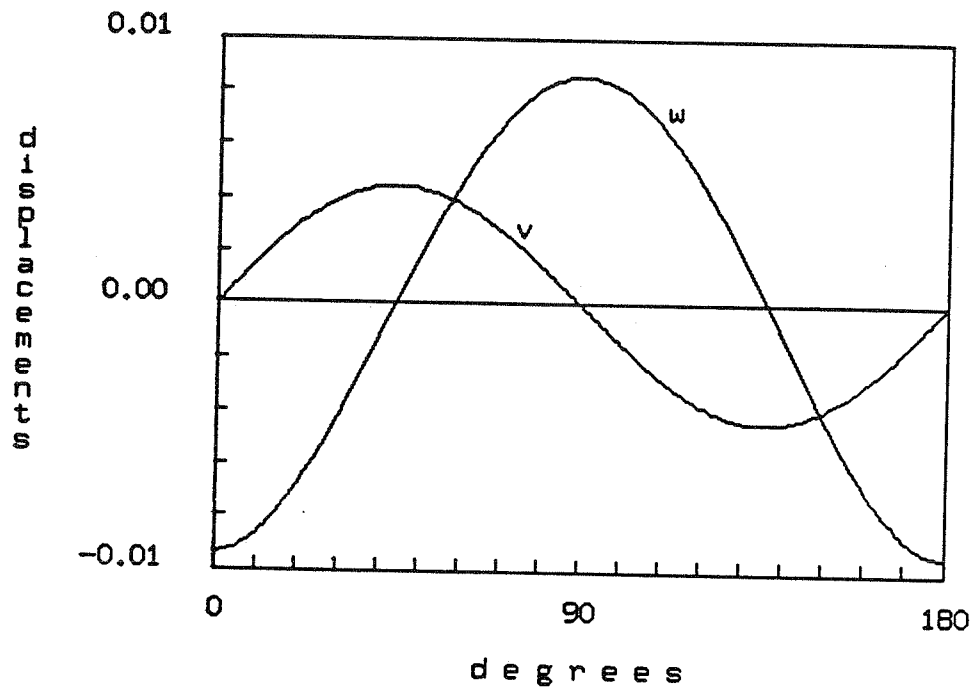


Fig.7.4. Displacements w_n and v_n of a pinched ring. $N = 100$.

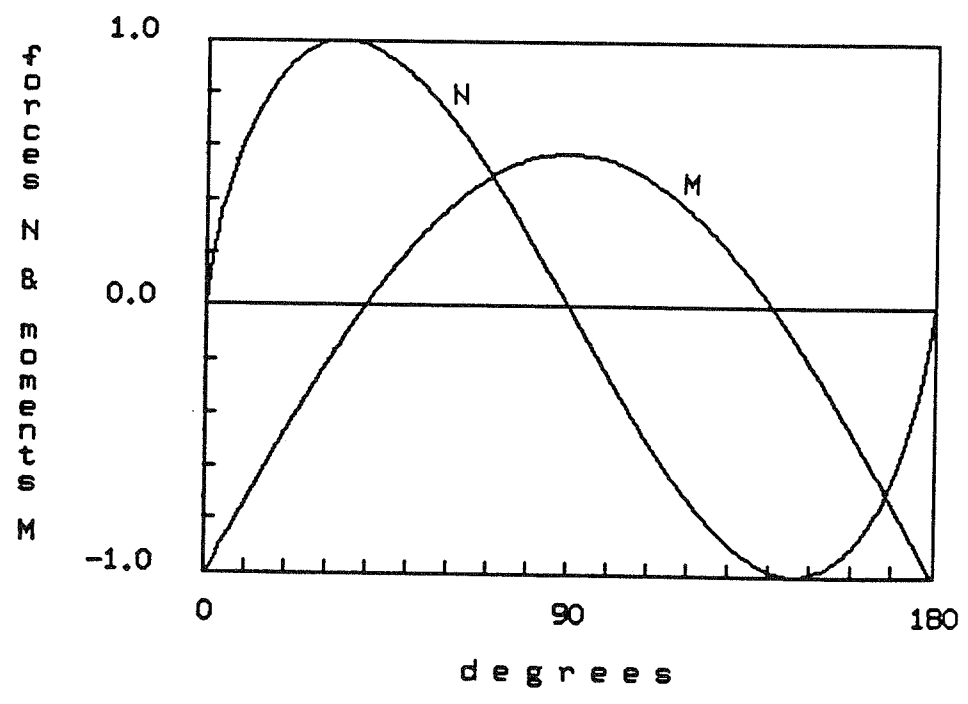


Fig.7.5. Normalized membrane forces N_n and internal moments M_n of a pinched ring. $N = 100$.

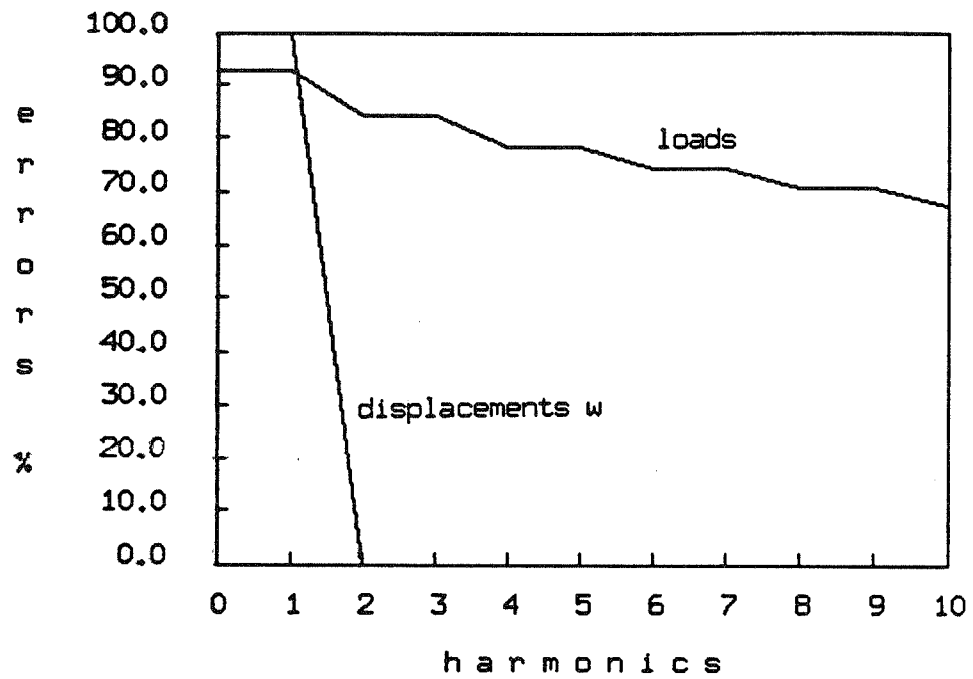


Fig.7.6. Spectral errors of loads and displacements w for two concentrated forces related to $N = 1000$.

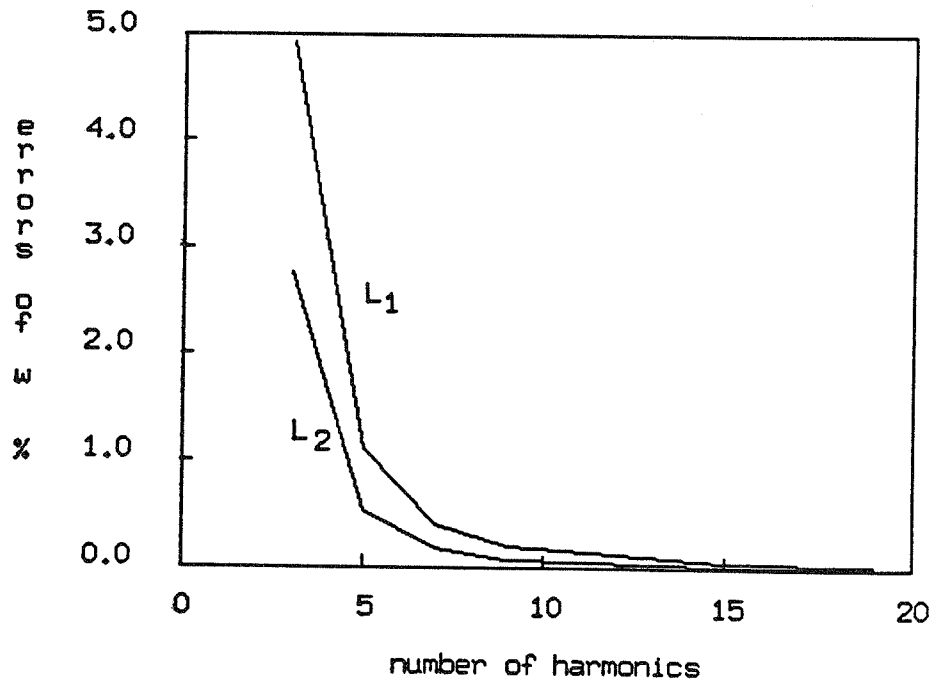


Fig.7.7. Errors of displacements w for two concentrated forces related to $N = 1000$ computed at control points.

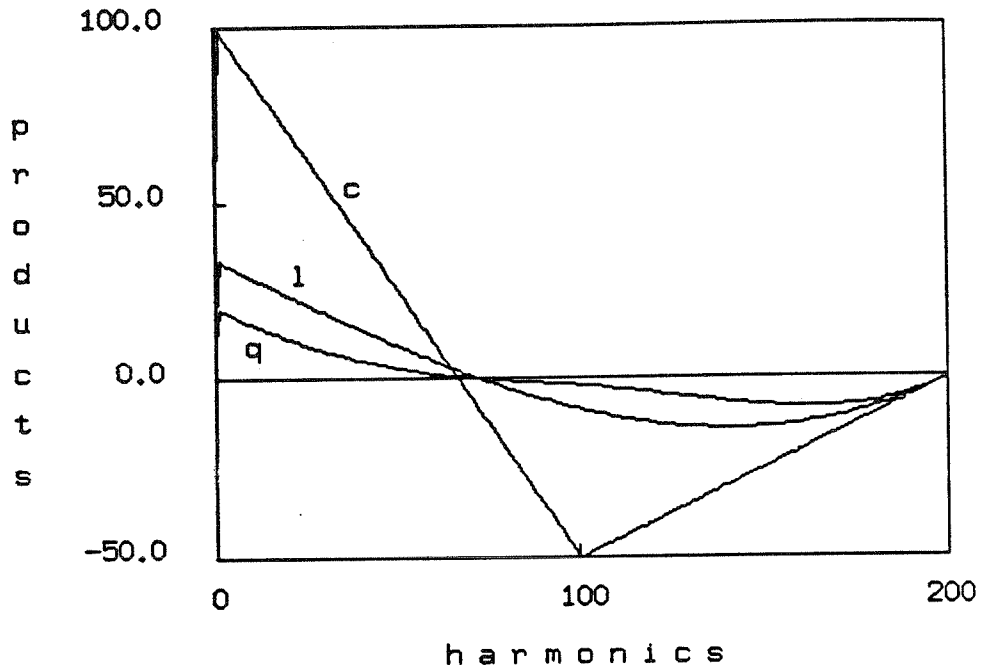


Fig.7.8.a. Spectrum of the product $a_n \sin n\phi * a_m \sin m\phi$ for $n, m = 0, 100$ for constant, linear and quadratic a_n .

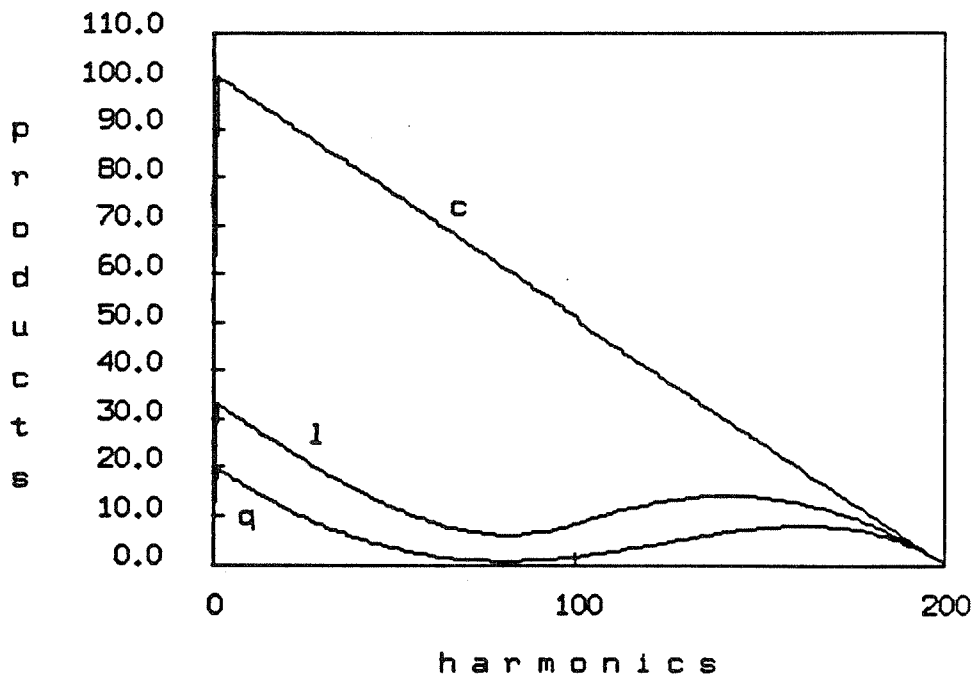


Fig.7.8.b. Spectrum of the product $a_n \cos n\phi * a_m \cos m\phi$ for $n, m = 0, 100$ for constant, linear and quadratic a_n .

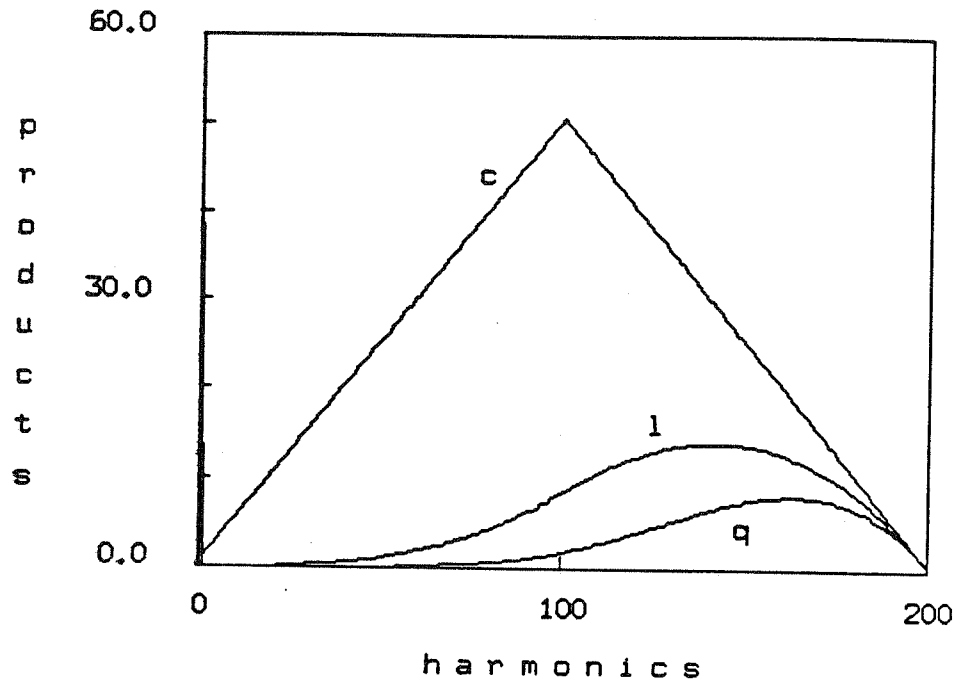


Fig.7.8.c. Spectrum of the product $a_n \sin n\phi * a_m \cos m\phi$ for $n, m = 0, 100$ for constant, linear and quadratic a_n .

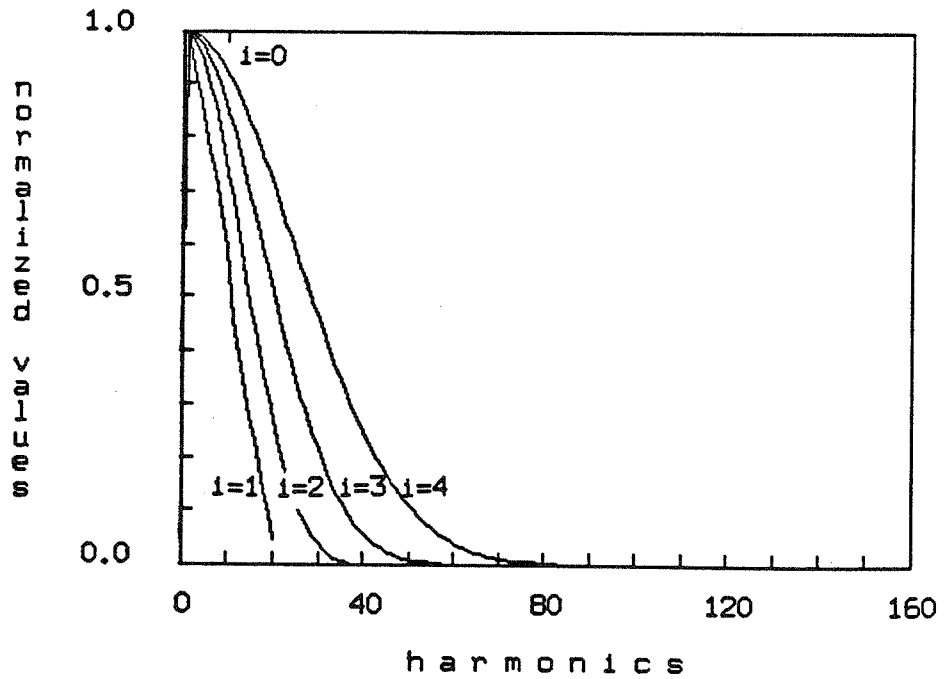


Fig.7.9. Normalized spectra for $f^i = f^{i-1} * f^{i-1}$ with $i = 1, 2, 3, 4$. $f^0 = \sum_{n=0}^{10} 1 \cos n\phi$.

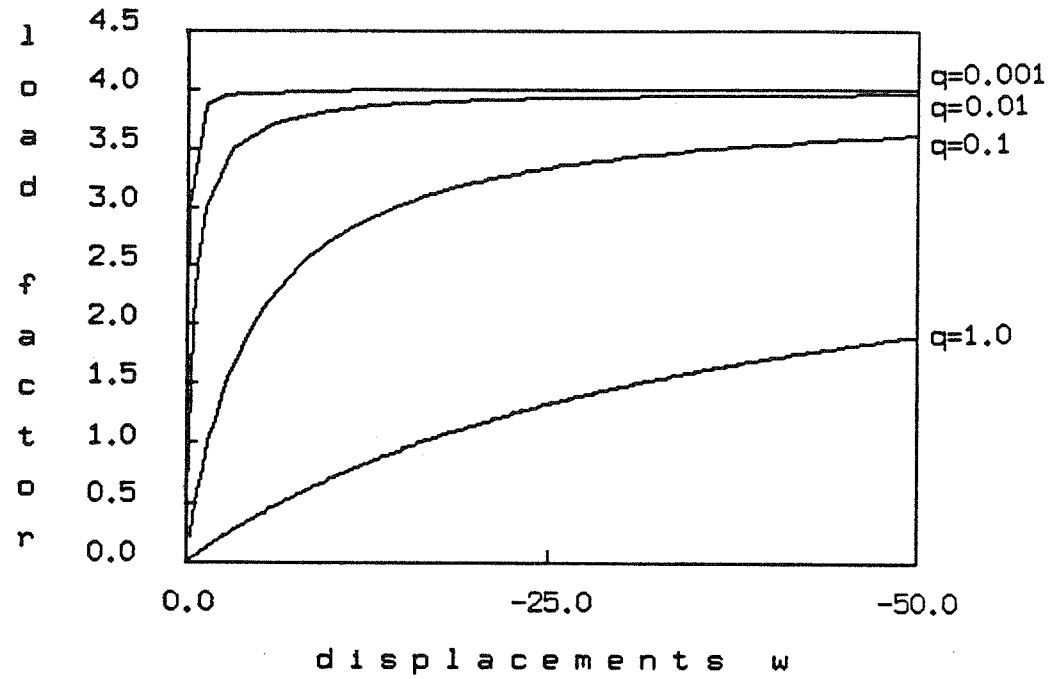


Fig.7.10. Load - displacement curves for ring (point $\phi = 0^\circ$) under loads $p_w = \alpha (1 + q \cos 2\phi)$, $q = 1.0, 0.1, 0.01, 0.001$.

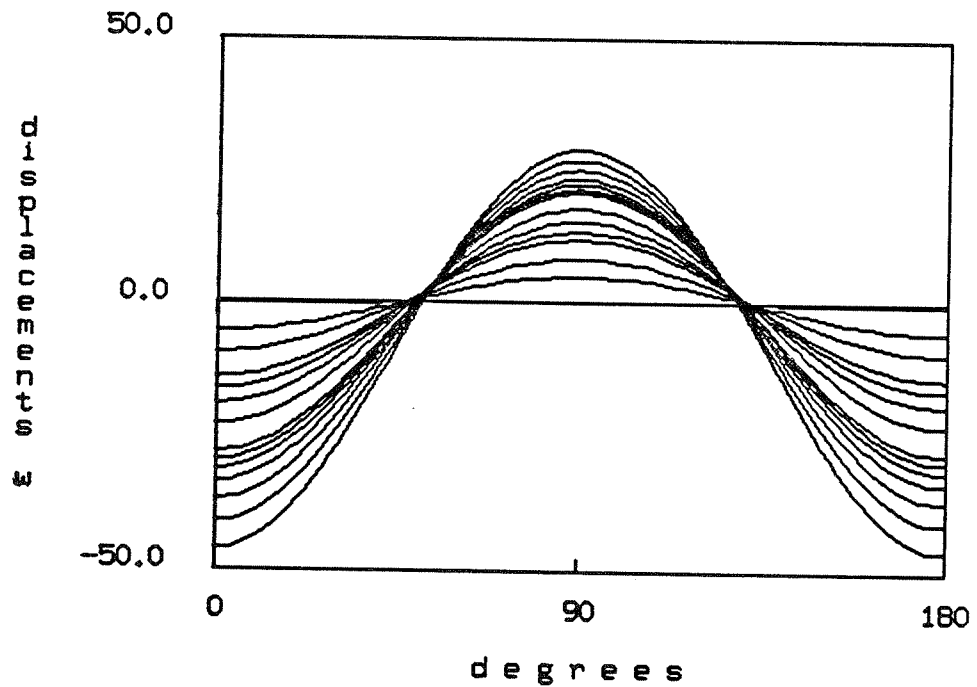


Fig.7.11. Displacements w of ring under loads $p_w = \alpha (1 + q \cos 2\phi)$ for $q = 0.001$.

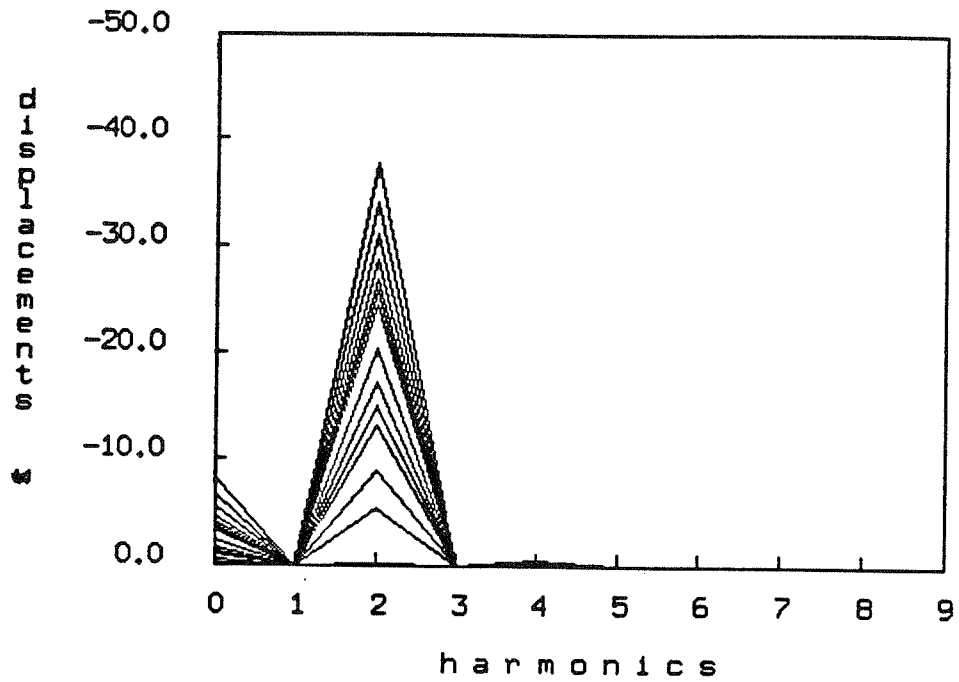


Fig.7.12. Spectral representations of displacements w of ring under loads $p_w = \alpha (1 + q \cos 2\phi)$ for $q = 0.001$.

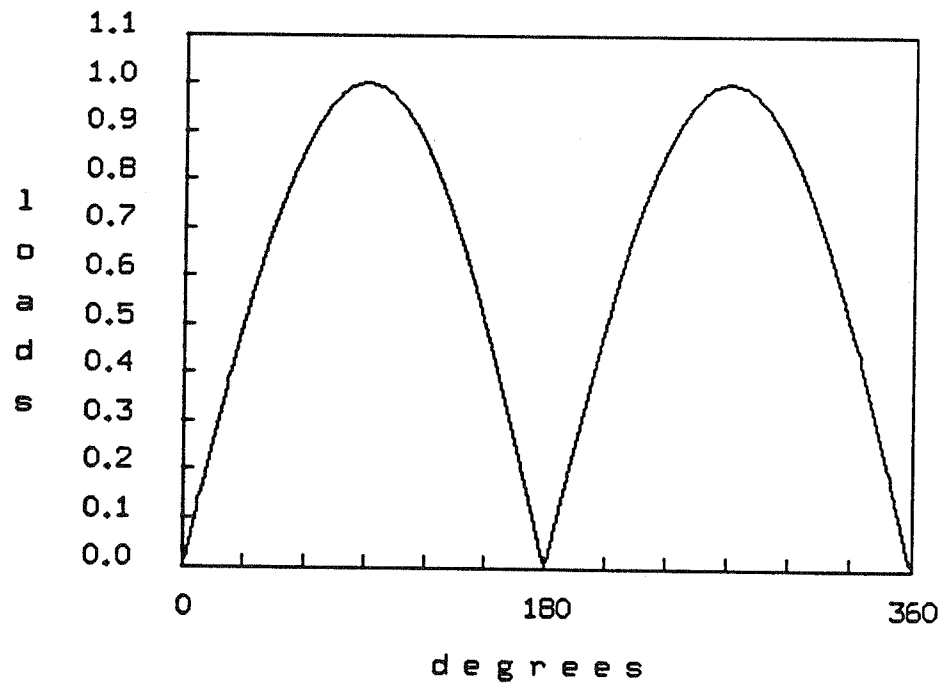


Fig.7.13. Loads $p_w \approx \sin\phi$ for $0 \leq \phi \leq \pi$.

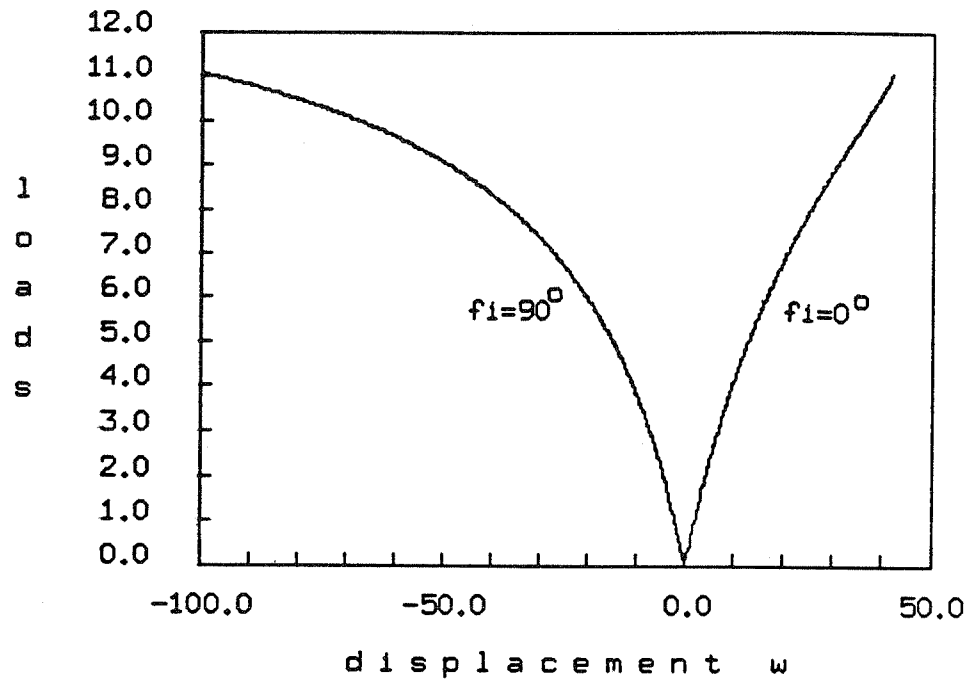


Fig.7.14. Load - displacement w curves for ring under loads $p_w \approx \sin\phi$. Points $\phi = 0^\circ$ and $\phi = 90^\circ$.

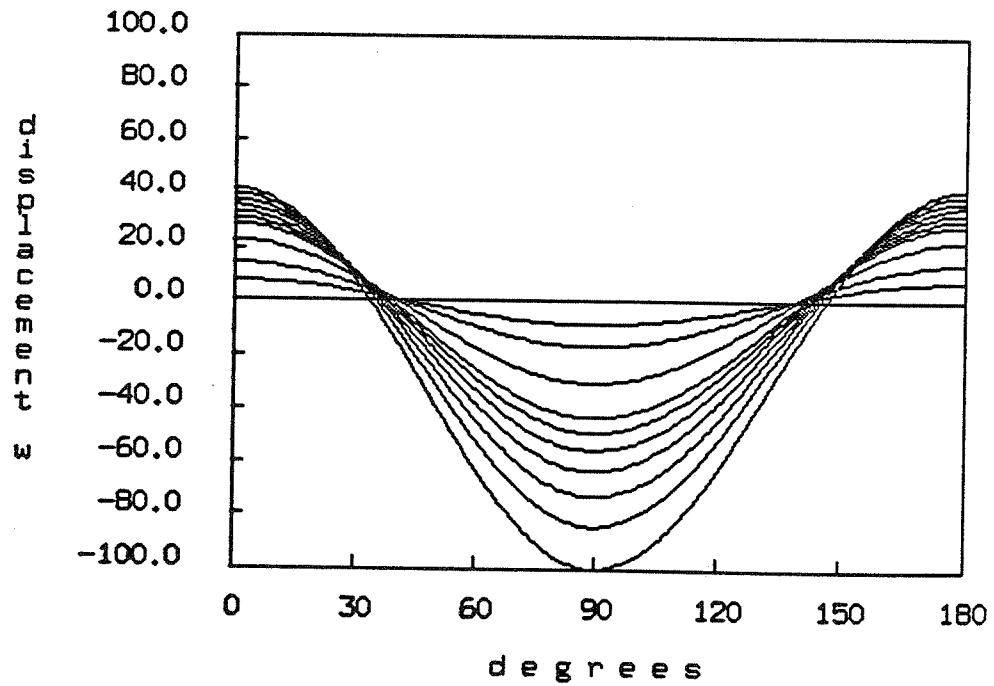


Fig.7.15. Displacements w of ring under loads $p_w \approx \sin\phi$.

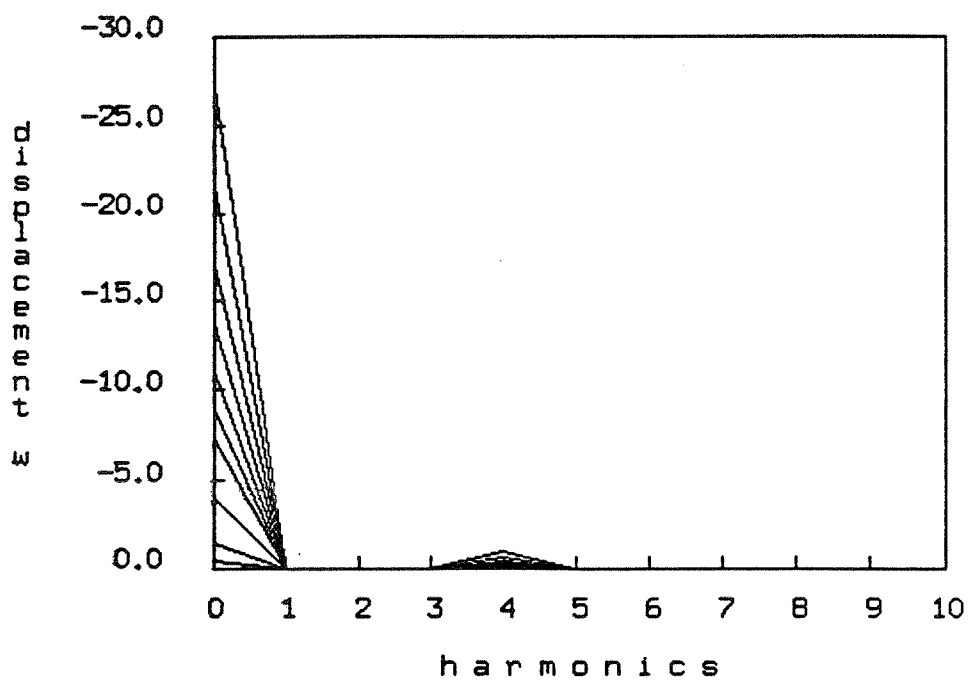


Fig.7.16. Spectral representation of displacements w_n of ring under loads $p_w \approx \sin \phi$.